

Contents list available at CBIORE journal website

International Journal of Renewable Energy Development

Journal homepage: https://ijred.cbiore.id



Research Article

Simulation model of active distribution network lines with high proportion distributed photovoltaic energy storage access

Di Zhai[®], Wenhua Ye[®], Ming Ma^{*}[®], Yunshu Deng[®], Jingchen Yang[®]

Yuxi Power Supply Bureau, Yunnan Power Grid Co., Ltd, Yuxi, 653100, China

Abstract. To address the voltage stability and power quality issues prevalent in active distribution lines with a significant proportion of distributed PV energy storage, the study proposes a novel multi-time reconfiguration loss reduction model for active distribution networks. This model employs a phased optimization strategy and a security-constrained optimal tidal current technique to enhance efficiency and reliability. The proposed method can effectively allocate reactive power output based on reactive power capacity, achieving better reactive voltage control. The nodes with a smaller reactive power capacity, nodes 2 and 3, exhibited an output of 0.33 Mvar. In comparison, the nodes with a medium capacity, nodes 27 and 28, demonstrated an output of 0.71 Mvar. Finally, the nodes with the largest capacity, nodes 16 and 17, exhibited an output of up to 0.98 Mvar. This differentiated reactive power allocation strategy effectively optimized voltage control and ensured the stability of active distribution network lines. In addition, the annual system operating cost of the suggested method was reduced by 167,889.33 yuan. From this, the proposed method demonstrates significant benefits in both economic and environmental aspects. It provides a practical and feasible optimization strategy for the high proportion of distributed photovoltaic energy storage connected to active distribution networks, which can promote the transformation of energy structure.

Keywords: High proportion distributed; Active distribution network; Multiple time periods; Refactoring and loss reduction; SOP



@ The author(s). Published by CBIORE. This is an open access article under the CC BY-SA license (http://creativecommons.org/licenses/by-sa/4.0/)
Received: 29th Sept 2024; Revised: 15th Dec 2025; Accepted: 21th January 2025; Available online: 15th Feb 2025.

1. Introduction

Faced with the intensification of environmental challenges, Renewable Energy (RE) has become crucial. Photovoltaic Power Generation (PPG), as a clean and RE source, has become a key factor in the global energy transition due to its minimal impact on the environment and wide range of energy sources (Zhou et al. 2023, Liu et al. 2024). However, the intermittency and instability of PPG pose significant challenges to the stability of the power grid (Furusawa et al. 2023). To address this challenge, researchers have proposed a solution of integrating Distributed Photovoltaic Energy Storage (DPV-ES) into the Distribution Network (DN), to smooth out the fluctuations of PPG through the energy storage system (Liu et al. 2024, Ge et al. 2022). Shah Shah et al (2021), developed an optimized scheduling model by combining DPV-ES with battery storage stations and microgrids to address the variability and prediction uncertainty of solar power generation. This model effectively alleviated the pressure faced by the public power grid due to the variability of PPG (Shah et al. 2021). Liao et al. (2024) proposed a clustering-based dual-layer optimization configuration method for DPV-ES systems. This method could effectively reduce voltage fluctuations at various nodes, minimize the risk of voltage exceeding limits, and reduce line loss rates (Liao et al. 2024). On the basis of considering the power grid and user demand, Yi et al. (2022) improved DPV-ES and proposed a multi-objective equilibrium optimization algorithm, which had advantages in convergence speed, selection ability, and population diversity. Xu et al (2022). innovatively used ice thermal storage technology and combined it with DPV-ES to study household air conditioning. Under different operating conditions, by optimizing the lower limit of solar irradiance, refrigerators could operate stably in various weather conditions, and the icemaking capacity increased by 40.91% (Xu et al. 2022). Lan et al. (2024) put forth a comprehensive distributed load frequency control scheme for multi-area power systems. To address the inherent challenges posed by the intermittent power generation characteristics of RE sources, the authors employed the powerful DPV-ES technology to enhance the analysis and control of power system frequency stability. The experimental results showed that the scheme demonstrated significant robustness to load disturbances and the intermittent nature of RE generation, effectively guaranteeing the stable operation of the power system (Lan et al. 2024). These studies not only demonstrate the potential of DPV-ES technology in improving grid stability and economic benefits but also point out the direction for future development.

Active DN refers to a power grid that achieves bidirectional energy flow and dynamic management by connecting distributed generation resources, energy storage devices, etc. based on traditional DN (Cong et al. 2024). This power grid structure can better adapt to the integration of DPV-ES, improve energy utilization efficiency, and reduce energy losses (Kaicheng et al. 2024). Currently, the research in active DN line optimization mainly focuses on two core areas: one is to reduce the energy loss of the power grid, and the other is to focus on

.

^{*}Corresponding author

improving the scheduling efficiency of the DN and optimizing its operation strategy (Adedayo et al. 2023, Velasco-Gómez et al. 2023). Liu et al. (2022) proposed a restoration capability enhancement strategy to address severe large-scale power outages in active DN under extreme ice and snow disasters. This strategy effectively shortened the power outage time, reduced the impact range of power outages, and improved the overall recovery efficiency of power grid lines, thereby significantly enhancing the reliability and stability of active DN lines (Liu et.al. 2022). Zheng et al. (2021) proposed an effective planning scheme to handle the issue of load expansion in active DN in large planning areas, in response to the shortcomings of load expansion in active DN. The proposed planning scheme was applicable and effective and could save more than 10% of investment (Zheng et al. 2021). Singh et al. (2021) proposed a distributed control strategy that could be coordinated with existing controllers to control the voltage of active DN lines within a specified range. This distributed control strategy not only effectively maintained the voltage within the specified safe range but also significantly improved the stability of active DN lines (Singh et al. 2021). Mukherjee et al. analyzed the optimal placement problem of Power Management Units (PMUs) in fully observable active DN and proposed a new objective function that considered the channel cost and operational risk of µPMUs at system nodes. The proposed method successfully reduced the total power supply cost by 13.21% and increased the redundancy measured by 2.44% (Mukherjee et al. 2022). Nemati et al. (2024) proposed a two-tier model based on active distribution grids to solve the uncertainty problem of RE generation and minimize the total cost of the microgrid by modeling the planning of generation and line extension. Experimental results showed that when the microgrid was able to exchange energy with other microgrids in a cooperative way, the model could achieve a cost reduction of 0.38% compared to the microgrid operator in a non-cooperative trading scenario (Nemati et al 2024).

In summary, with the continuous increase in the penetration rate of RE in active DN, the power grid is facing the challenge of balancing the penetration rate and stability of RE. Despite the numerous optimization methods proposed by industry scholars, the existing solutions remain challenging to fully adapt to the complexities of power systems, particularly in ensuring safe and cost-effective operations, addressing the intermittency of renewable energy sources, and accounting for the inherent uncertainty in generation capacity and load. Therefore, it is necessary to fully consider the impact of RE generation capacity and uncertain load changes. These factors, when considered collectively, represent the fundamental challenge of optimizing the operation of the power grid. However, existing methods still have limitations in addressing these issues and have not fully met practical needs. In response

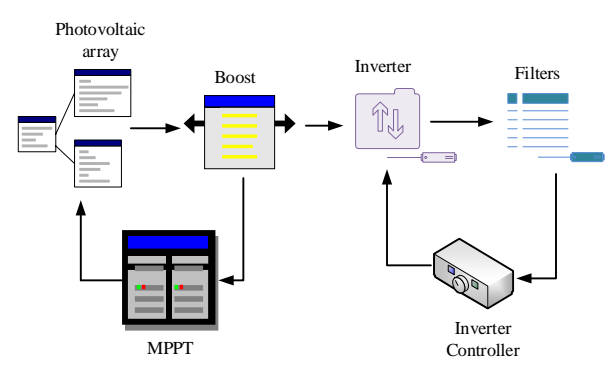


Fig 1 High-Proportion DPV-ES Grid-Connected System Structure

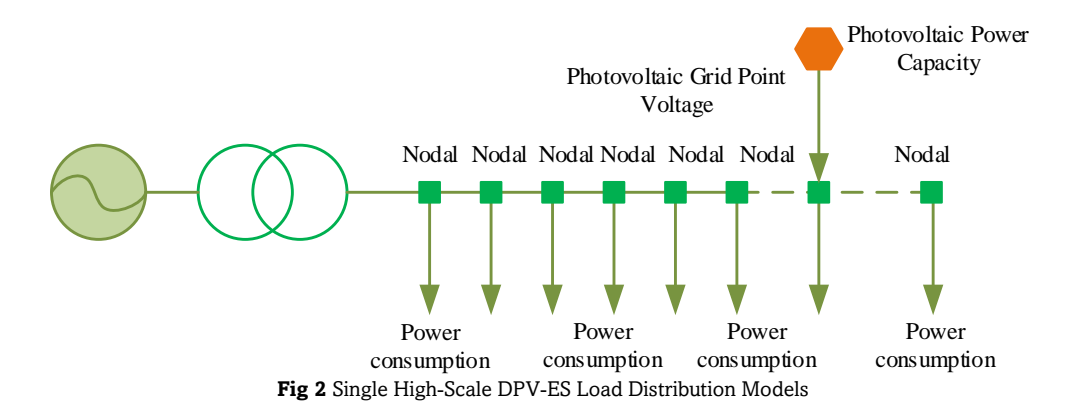
to this challenge, this study innovatively integrates high-proportion DPV-ES into active DN lines and establishes a multiperiod reconstruction loss reduction model for DN with high-proportion DPV-ES integration. Based on Security Constrained Optimal Power Flow (SOP), an SOP-based multi-period reconstruction loss reduction model for active DN is constructed. This study aims to enhance the performance of active DN lines through innovative methods, improving energy efficiency and system stability.

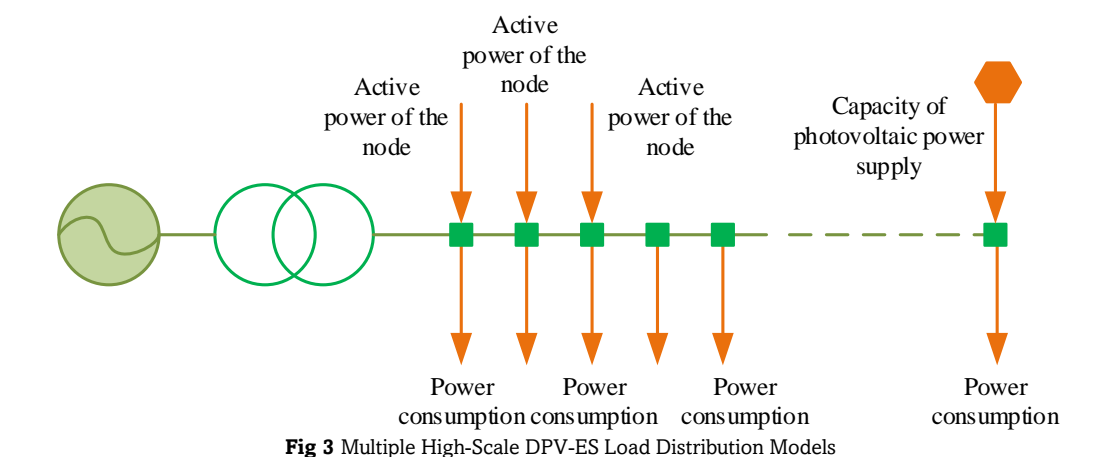
2. Methods

2.1 The impact of high-proportion DPV-ES access on the voltage of active DN

In contemporary power systems, the accelerated development and reduction in the cost of DPV-ES has resulted in a significant increase in the proportion of DPV-ES connected to DN (Sun *et al.* 2021; Bandewad *et al.* 2023). The selected access method will have a notable effect on the voltage stability and power quality of the DN (Liao *et al.* 2021; Novoa *et al.* 2021). Therefore, analyzing the impact of high proportion DPV-ES access on the voltage of active DN is essential. The structure of the high-proportion DPV-ES grid-connected system is shown in Figure 1.

In Figure 1, the high-proportion DPV-ES grid-connected system is a power generation system. It consists of a photovoltaic array, a Maximum Power Point Tracking (MPPT) controller, a Boost converter, an inverter, a filter, and a two-stage controller (Dao *et al.* 2023; Bolgaryn *et al.* 2023). The photovoltaic array is responsible for collecting solar energy and converting it into direct current, which is then passed through an MPPT controller to maximize energy capture. Boost converters boost DC voltage, while inverters convert DC power into AC power for grid-connection. Filters are used to remove unnecessary noise from AC power and ensure power quality.





The first and second-level controllers work together to monitor and optimize the system, ensuring stable and efficient operation. Figure 2 illustrates the load distribution model when a single high-proportion DPV-ES is related to the active DN line.

In Figure 2, after a single high-proportion DPV-ES is introduced into the active DN, its photovoltaic capacity and access point location will become key factors affecting the voltage of each node. Under the premise of a constant initial voltage at the line, the connection of photovoltaic power sources will cause an increase in user voltage at the upstream node of the grid connection point. This increase is correlated with many various factors. When the connected photovoltaic system has a large capacity, the access point is located at the end of the power grid, and the user load is low, the amplitude of voltage rise is more significant. On the contrary, when the photovoltaic capacity is small, the access point is close to the starting end of the line, and the user load is high, the voltage rise amplitude is relatively small. The voltage at the photovoltaic grid-connection point U_p is calculated using equation (1).

$$U_{p} = U_{o} - \sum_{k=1}^{p} \frac{\left(\sum_{n=k}^{N} p_{n} - p_{v}\right) r l_{k}}{U_{k-1}} + \sum_{k=1}^{p} \sum_{n=k}^{N} Q_{v} x l_{k}$$
(1)

In equation (1), p_n and p_v respectively represent the active power and photovoltaic power capacity of the node. r and l_k

respectively represent the resistance per unit length and the distance between two nodes. Q_v and x respectively represent reactive power and unit reactance. U_o and U_{k-1} represent different node voltages. The load distribution model when multiple high proportion DPV-ES are connected to the source DN line is shown in Figure 3.

In Figure 3, after connecting multiple high proportion DPV-ES in the active DN line, the line voltage will be significantly affected. The key factors affecting voltage changes include the installed capacity of high proportion DPV-ES, the specific location of the access point in the power grid, and the user's electricity load. Among these factors, the power generation output of photovoltaic power sources exerts a particularly notable influence on the voltage trend of the DN. This, in turn, affects the amount of energy injected into the grid, thereby determining the changes in voltage levels. The calculation expression for the node voltage U_m after the high-proportion DPV-ES is shown in equation (2).

$$U_{m} = U_{o} - \sum_{k=1}^{m} \frac{\left(\sum_{n=k}^{N} p_{n} - p_{vn}\right) r l_{k} + \sum_{n=k}^{N} Q_{n} x l_{k}}{U_{k-1}}$$
(2)

In equation (2), p_{vn} denotes the capacity of the n-th load node connected to the photovoltaic power source.

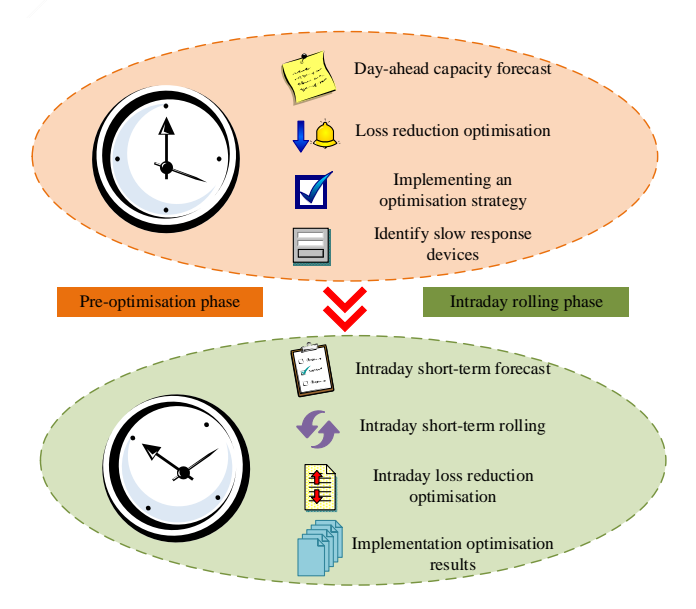


Fig 4 Structure of a Two-Phase Coordinated Loss Reduction Method for Active DN

2.2 Two stages coordinated loss reduction method for active DN with high-proportion DPV-ES access

Based on the above analysis, when a high proportion of DPV-ES is introduced into active DN lines, the active output of new energy will cause a significant increase in voltage on the lines. The magnitude of this increase is related to the size of the active output and the position of the connection point. The higher the output power and the later the location of the connection point, the greater the voltage increase on the lines. However, the insufficient prediction accuracy of PPG output limits the accuracy of system regulation (Hu et al. 2023, Hu et al. 2022, Hou et al. 2024). Therefore, it is crucial to develop refined coordinated optimization control methods for active DN. With this situation, a phased optimization strategy is proposed, which is a two-stage coordinated loss reduction method for active DN with high-proportion DPV-ES access. The structural framework of this method is shown in Figure 4.

In Figure 4, the phased optimization strategy proposed in the study focuses on the coordinated optimization of the active DN in two phases, namely the day-ahead optimization phase and the intra-day rolling phase. The day-ahead optimization phase focuses on developing an initial grid operation plan based on forecast data to ensure efficient grid layout and equipment capacity planning in the initial phase. The intra-day rolling phase adjusts and optimizes the grid operation with real-time data to accommodate the volatility and uncertainty of new energy output. In addition, the strategy uses in-depth analysis of historical trends and forecasting models in the day-ahead optimization phase to determine the optimal configuration and installed capacity of grid equipment to minimize economic and environmental costs. The intra-day rolling phase then fine-tunes grid operations through real-time monitoring and rapid response mechanisms to ensure that the grid can instantly adapt to changes in external conditions, such as weather changes and load fluctuations. This two-phase strategy not only improves the flexibility and adaptability of grid operation but also helps to achieve more efficient energy distribution and loss reduction. The objective function calculation equation for the recent optimization phase is shown in equation (3).

$$\begin{cases} f_{eco} = E_{p,t} \times \sum_{(i,j) \in N}^{t=1} p_{grid,j,t} \\ f_s = \sum_{(i,j) \in N}^{t=1} I_{ij,t} \times r_{ij} \\ f_{vol} = \sum_{i \in N}^{i=1} (v_i - v_{adm}) \end{cases}$$

$$(3)$$

In equation (3), f_{eco} , f_s , and f_{vol} respectively represent the

sum of purchase cost, network loss, and voltage squared deviation. $E_{p,t}$ and $I_{ij,t}$ respectively represent the unit electricity price and the square of current of branch ij at time $t.\ r_{ij}$ represents the resistance of branch $ij.\ p_{grid,j,t}$ represents the active power purchased from the grid. ν_i and ν_{adm} respectively represent the node voltage and the square of the maximum allowable operating voltage. The constraint expression for the optimization stage is shown in equation (4).

$$\begin{cases} v_{i,\min} \le v_{i,t} \le v_{i,\max} \\ 0 \le l_{ij,t} \le l_{ij,\max} \end{cases} \tag{4}$$

In equation (4), $v_{i,min}$ and $v_{i,max}$ are the square of the lower and upper limits of the node voltage. $l_{ij,max}$ represents the square of the maximum branch current. The objective function for the intra-day rolling phase $min f^{RN}$ is shown in equation (5).

$$\begin{cases}
\min f^{RN} = \sum_{\tau=1} p_{WS,\tau}^{NR} \\
P_{WS}^{NR} = \sum_{t=1}^{T^{RN}} l_{ij,t} R_{ij,tt}
\end{cases} \tag{5}$$

In equation (5), $p_{WS,\tau}^{NR}$ represents the network loss of a single optimization. N and τ respectively, represent the set of branches and the number of rolling times. tt represents the time variable of the rolling stage within the day. Distributed Power Flow (Distflow) is a power flow calculation method designed for large-scale distributed generation systems. It considers the geographical dispersion and small-scale characteristics of distributed generation resources and can more accurately simulate and analyze the power flow in modern DN (Igor $et\ al.\ 2023$; Hirano $et\ al.\ 2022$; Ning 2022). Therefore, the study adopts the Distflow model to describe the power flow of radial DN lines. The calculation equation for the head power of the branch S_{ij} is shown in equation (6).

$$S_{ii} = V_i I_{ii}^*, \forall (i, j) \in D \tag{6}$$

In equation (6), V_i and I_{ij}^* are the conjugate of the head node voltage and the branch current, respectively.

2.3 Construction of Multi-period Reconstruction Loss Reduction Model for Active DN Based on SOP

The two-stage coordinated loss reduction method for active DN with high-proportion DPV-ES access proposed in the study effectively alleviates the related problems caused by the volatility and uncertainty of new energy. However, in the face of

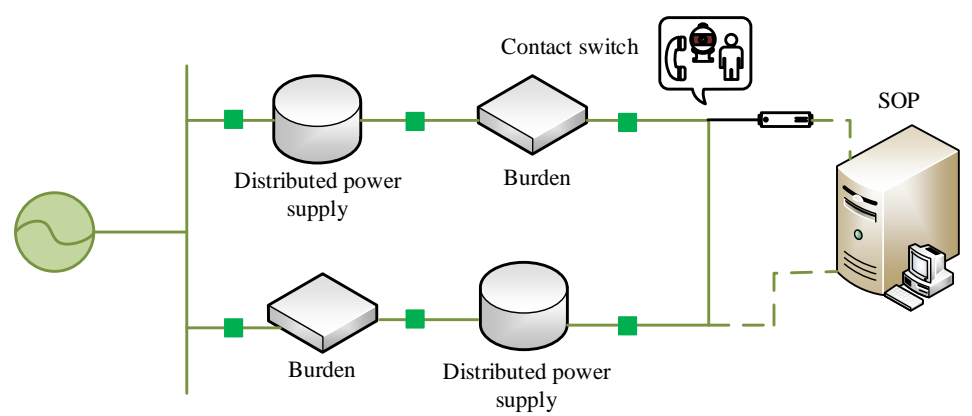


Fig 5 Location of SOP Access to the Active DN

a high proportion of DPV-ES access, how to consider intelligent soft switches and achieve multi-period optimization and reconstruction of active DN remains an urgent issue in the current research field (Liu *et al.* 2024, Xu *et al.* 2021). SOP is a method for optimizing power flow while considering system safety constraints in the operation of power systems (Prasad 2022, Ma *et al.* 2024). Its main goal is to achieve optimal economy, reliability, and power quality (Pan *et al.* 2024, Ebrahimi *et al.* 2024). Therefore, based on the two-stage coordinated loss reduction method for active DN with a high-proportion of DPV-ES access, this study introduces SOP and proposes a new SOP-based multi-period reconstruction loss reduction model for active DN. The location of SOP about the active DN is illustrated in Figure 5.

In Figure 5, in the active DN lines with high proportion DPV-ES access, this study installs SOP between adjacent feeders to replace traditional switches, to achieve more accurate management. In addition, SOP effectively reduces equipment wear and failure risks caused by switch actions by reducing frequent operations. Under standard operating conditions, the PQ-VdcQ control strategy is selected to manage the SOP intelligent soft switch. The expression for calculating the active power constraint of SOP under this control strategy is shown in equation (7).

$$P_i^{sop} + P_i^{sop,N} + P_j^{sop} + P_j^{sop,N} = 0 (7)$$

In equation (7), P_i^{sop} and $P_i^{sop,N}$ respectively are the active power and active loss transmitted by SOP at node $i.P_j^{sop}$ and $P_j^{sop,N}$ are the active power and active loss transmitted by SOP at node j. The expression for calculating the reactive power constraint of SOP is shown in equation (8).

$$\begin{cases} Q_{i,\min}^{sop} \leq Q_i^{sop} \leq Q_{i,\max}^{sop} \\ Q_{j,\min}^{sop} \leq Q_j^{sop} \leq Q_{j,\max}^{sop} \end{cases}$$
(8)

In equation (8), $Q_{i,min}^{sop}$ and $Q_{i,max}^{sop}$ respectively represent the minimum and maximum reactive power transmitted by SOP at node $i.Q_{j,min}^{sop}$ and $Q_{j,max}^{sop}$ respectively represent the minimum and maximum reactive power transmitted by node j. The SOP

capacity constraint calculation expression is shown in equation (9).

$$\sqrt{(p_i^{sop})^2 + (Q_i^{sop})^2} \le S_i^{sop} \tag{9}$$

In equation (9), S_i^{sop} represents the rated capacity of the SOP converter. The expression for calculating the objective function $\min F$ is shown in equation (10).

$$\min F = W_1 \Box (f_1 + f_2) + W_2 \Box f_3 \tag{10}$$

In equation (10), W_1 and W_2 represent weight coefficients. f_1 , f_2 , and f_3 respectively represent the deviation degree of power loss cost, switch operation cost, and node voltage. The calculation equation for switch frequency constraint is shown in equation (11).

$$\sum_{i \in \mathcal{S}} \left| \lambda_{ij} - \lambda_{ij,0} \right| \le \varpi_b^{all} \tag{11}$$

In equation (11), λ_{ij} and $\lambda_{ij,0}$ represent the status of the interconnection switch and the disconnection status of the branch, respectively. $\lambda_{ij,0}$ represents the maximum allowable number of disconnections for all switches. The constraints on connectivity and radiation are expressed in equation (12).

$$\begin{cases} \sum_{j=1}^{N} \sigma_{ij} = 1\\ \sigma_{ij} = 0 \end{cases}$$
 (12)

In equation (12), N and σ_{ij} are the number of system nodes and the initial contact switch state variables of the network, when node i is the upper-level node of node j, σ_{ij} is 1. If it is the lower level node, σ_{ij} is 0.

3. Results

3.1 Simulation Testing of Two-Stage Coordination Method for Active

To test the performance of the method proposed by this study, a suitable experimental environment was established. The IEEE

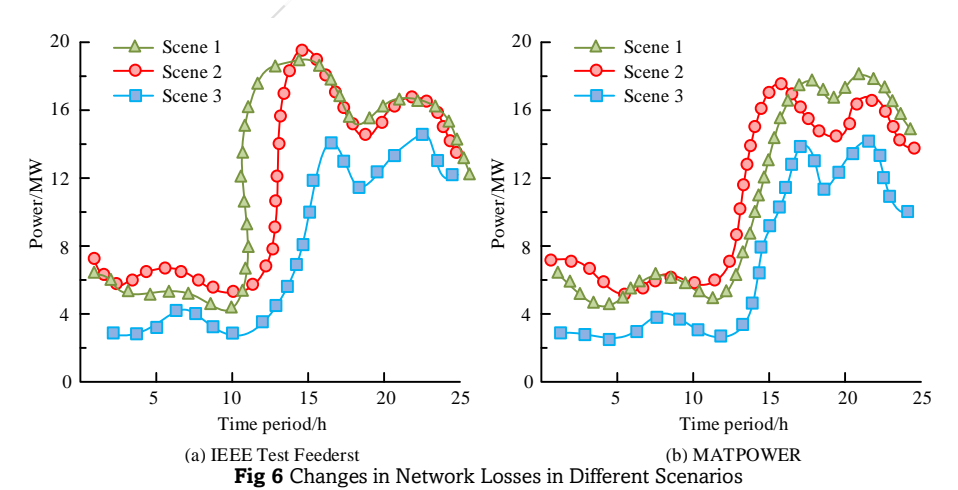


Table 1
Specific Parameter Settings

specific Farameter Settings								
Parameters	Discrete variable			Continuous variable				
	SC1/kVar	SC2/kVar	OLTC	SC3/kVar	SC4/kVar	SVC/kVar		
Adjustment range	0-220	0-220	0.90-1.05	0-220	0-220	49.05		
Pacemaker	50	50	0.01	50	50	/		
Gear level	/	/	±5	/	/	/		
Access node	5	10	1	17	30	6,18		

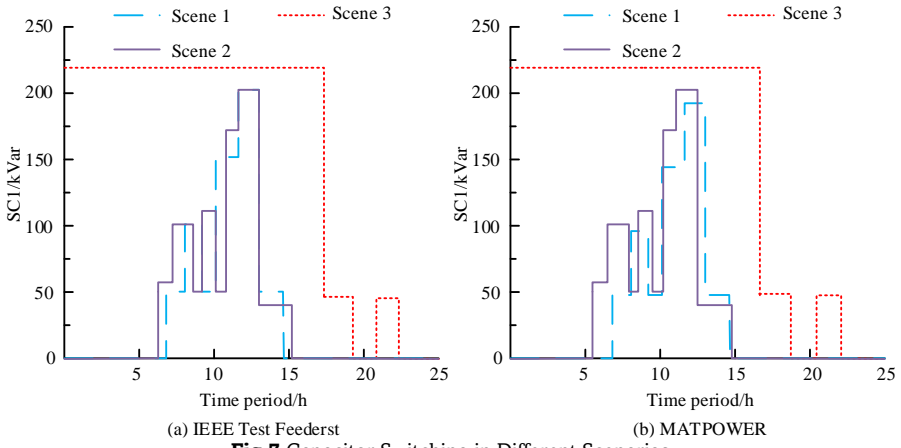
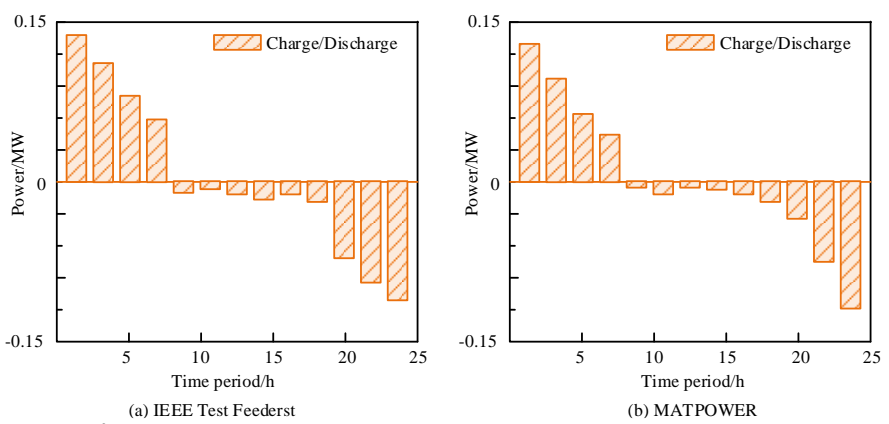


Fig 7 Capacitor Switching in Different Scenarios



 $\textbf{Fig 8} \ \text{Charging and Discharging of Energy Storage During the Intraday Phase}$

33 node system was adopted for simulation testing, and the IEEE Test Feederst dataset and MATPOWER dataset were used as test data sources. Table 1 illustrates the particular parameter settings.

This study arranged three experimental scenarios based on the parameter settings in Table 1: Scene 1 and Scene 2 were traditional optimization strategies, namely reactive power optimization loss reduction method (Raju *et al.* 2024) and active power optimization loss reduction method (Venkatesan *et al.* 2021); Scene 3 was the two-stage coordinated loss reduction method for active DN with the proposed high-proportion DPV-ES access. The study first compared the hourly network loss changes in three scenarios. The test results are shown in Figure 6

In Figure 6, whether in the IEEE Test Feederst dataset or the MATPOWER dataset, Scene 3 shows superior performance in reducing network loss compared to Scenes 1 and 2. Especially at night and dawn, PPG produced almost no electricity output, and the benefits of comprehensive control strategies in reducing grid losses were particularly significant. From this, the comprehensive control of active and reactive power loss reduction strategies exhibited better efficiency compared to individual active or reactive power loss reduction methods. This emphasized the importance of two-stage coordinated control for optimizing grid performance during low PPG periods. This result is consistent with the conclusion reached by Cong et al. (Cong et al. 2024). In Figure 7, the study also compared the switching of capacitors in different scenarios.

In Figure 7 (a), during the time period from 6:00 to 13:00,

the number of C1 switches in Scene 3 was significantly less than that in Scene 1 and Scene 2, both of which switched 7 times, while Scene 3 only switched 1 time. In Figure 7 (b), C1 in Scene 1 and Scene 2 were switched 7 and 8 times respectively, while Scene 3 remained the lowest with only 1 switch. This indicated that in the application of active DN line loss reduction, the two-stage coordinated control strategy was not only effective but also significantly reduced the switching frequency of discrete capacitors, prolongs their service life, and enhanced the economic efficiency of operation. In Figure 8, to verify the energy storage effect of the two-stage coordinated loss reduction method for active DN with the proposed high-proportion of DPV-ES access, the daily stage energy storage charging and discharging situation was also tested.

Figure 8 (a) shows the daily energy storage charging and discharging situation of the two-stage coordinated loss reduction method for active DN with high proportion DPV-ES access in the IEEE Test Feederst dataset. Figure 8 (b) shows the daily energy storage charging and discharging situation of the two-stage coordinated loss reduction method for active DN with high proportion DPV-ES access in the MATPOWER dataset. Due to the emphasis on refined management in the daily optimization strategy to adapt to the impact of new energy on the power grid, this study specifically conducted detailed regulation on devices such as energy storage systems that can respond quickly. In Figure 8, whether in the IEEE Test Feederst dataset or the MATPOWER dataset, the energy storage devices mainly performed discharge operations during the time period from 19:00 to 24:00 in the evening. This behavior was consistent

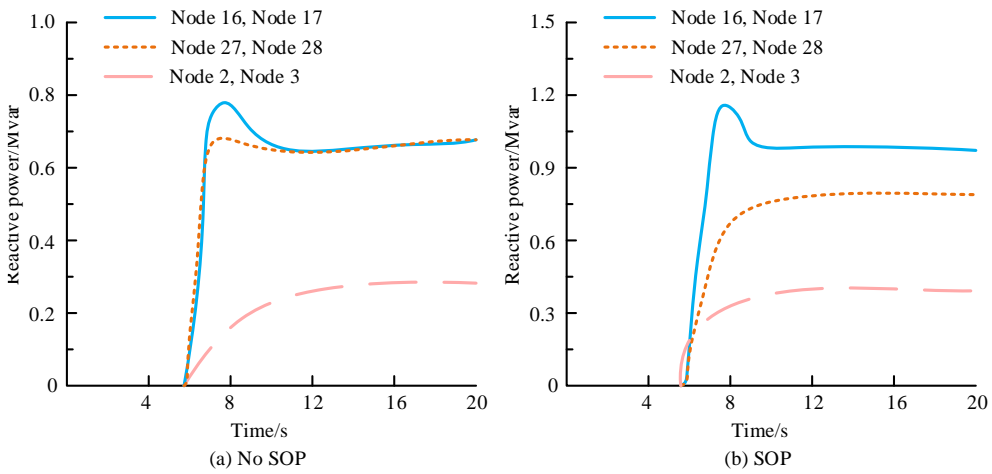


Fig 9 Transmission of the SOP

with the operating characteristics of the power grid during this period due to the decrease in new energy generation and the increase in electricity demand, reflecting the efficiency and adaptability of refined optimization strategies in reducing losses.

3.2 Simulation testing of multi-period reconstruction and loss reduction model for active DN

This study used the parameters listed in Table 1 to simulate and verify the multi-period reconstruction loss reduction model of active DN based on SOP. The photovoltaic reactive power output changes of the multi-period reconstruction loss reduction model for active DN without SOP and the multi-period reconstruction loss reduction model for active DN based on SOP are shown in Figure 9.

In Figure 9(a), in the multi-period reconstruction loss reduction model of an active DN without SOP, if there was

sufficient reactive power, the reactive power output of the high proportion DPV-ES was basically equal, both being 0.63Mvar. If the reactive power was insufficient, excessive droop gain would limit the reactive power output of the photovoltaic inverter, resulting in a low value of 0.28Mvar for its reactive power output. In Figure 9(b), in the SOP-based active DN multi-period reconstruction loss reduction model, nodes 2 and 3 with smaller reactive power capacity output 0.33Mvar, nodes 27 and 28 with medium capacity output 0.71Mvar, and nodes 16 and 17 with larger capacity output up to 0.98Mvar. The above experimental data indicated that SOP could more effectively allocate reactive power output based on reactive capacity, achieving better reactive voltage control. This study connected a high proportion of DPV-ES to nodes 5, 10, 15, 20, 23, and 32 of the DN. Taking a typical summer day in a certain region of China as an example, the voltage changes of each photovoltaic access point in the 24hour system were plotted, as shown in Figure 10.

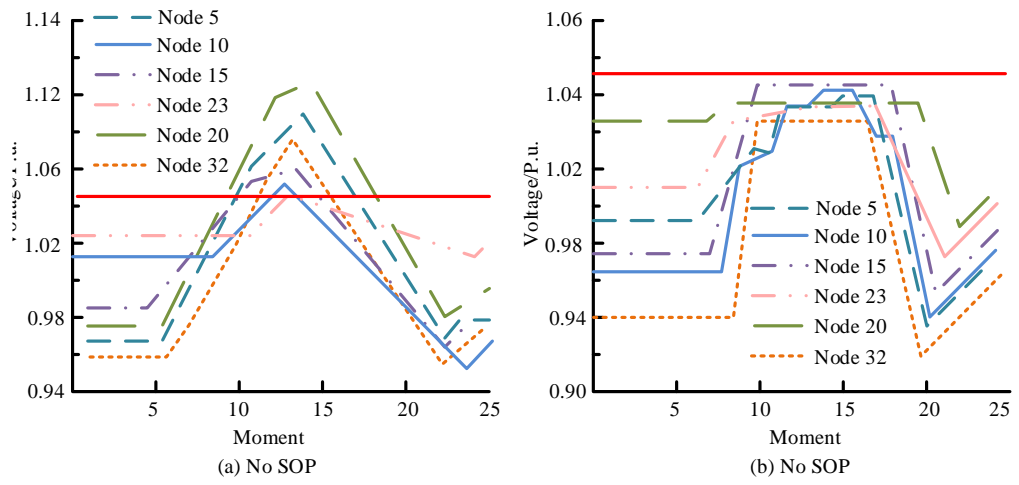


Fig 10 Generation Output and Load Variation Curves for High Ratio DPV-ES

Table 2Cost-effectiveness of Each Parameter

Cost-benefit analysis	SOP	No SOP	Decrease
Annual electricity loss cost/\$	122145.13	232514.63	110369.50
Annual switching costs/\$	5213.65	82056.13	76842.48
Annual SOP maintenance costs/\$	20215.63	0	-20215.63
Total annual system operating costs/\$	142147.36	310036.69	167889.33

Figure 10(a) illustrates the impact of adopting the multiperiod reconstruction loss reduction model of the active DN without SOP on the voltage at each grid-connection point. As the active output of the photovoltaic inverter increased, the voltage at each grid connection point generally rose, reaching its peak at 12-15. At this point, the probability of exceeding the voltage limit was approximately 18%. The peak voltage often occurred at the point of maximum active output, especially at the end photovoltaic node, where the voltage amplitude reached 1.126 p.u., far exceeding the specified range. In Figure 10 (b), after adopting the proposed SOP-based active DN multi-period reconstruction loss reduction model, although the increase in active output of the photovoltaic inverter still led to an increase in grid voltage, the voltage rise amplitude was effectively controlled through SOP control. This ensured that the voltage value remained within the allowable range and demonstrated a relatively ideal control effect. Finally, in Table 2, the study compared and tested the multi-period reconstruction loss reduction model of active DN without SOP with the SOP based model, using cost-effectiveness as the indicator.

In Table 2, the proposed SOP-based active DN multitemporal reconfiguration loss reduction model had better economic benefits. The annual system operating cost of the SOP-based active DN multi-temporal reconfiguration loss reduction model was reduced by \$167,889.33 compared to the active DN multi-temporal reconfiguration loss reduction model without SOP. Although the initial investment cost of SOP was high and the payback period was expected to be 15 years, the economic advantages of the SOP model would become more obvious as the cost of power electronic devices continued to decrease. In addition, from a long-term perspective, the SOP model could not only effectively reduce operating costs but also significantly improve the reliability and power quality of the grid by optimizing the grid operation strategy. This optimized-grid operation helped to reduce energy losses and improve the efficiency of power transmission, thus bringing double benefits at the economic and environmental levels, further highlighting the foresight and practicality of the SOP model. This conclusion is in line with that reached by Li et al. (2024).

4. Conclusion

Currently, the large-scale integration of DPV-ES has brought revolutionary changes to the DN. However, the high-proportion of DPV-ES access also poses significant challenges to the stable and optimized operation of active DN. Based on this situation, the study first analyzed the impact of high-proportion DPV-ES access on the voltage of active DN and proposed a two-stage coordinated loss reduction method for active DN with highproportion DPV-ES access. Secondly, based on the two-stage coordinated loss reduction method for active DN with a highproportion of DPV-ES access, SOP was introduced. Finally, an SOP-based multi-period reconstruction loss reduction model for active DN was built. Whether in the IEEE Test Feederst dataset or the MATPOWER dataset, the proposed method significantly reduced the number of capacitor switching times, requiring only one, thereby reducing operating costs and improving system reliability. In the multi-period reconstruction loss reduction model of active DN based on SOP, nodes 2 and 3 with smaller reactive power capacity output 0.33Mvar, nodes 27 and 28 with medium capacity output 0.71Mvar, and nodes 16 and 17 with larger capacity output up to 0.98Mvar. In addition, after adopting the proposed SOP-based active DN multi-period reconstruction loss reduction model, the voltage rise amplitude of each photovoltaic access point was effectively controlled,

ensuring that the voltage value remained stable within the allowable range. From this, the method proposed in the study is not only innovative in theory but also demonstrates high efficiency and practicality in practical applications. However, the proposed method mainly relies on high-proportion DPV-ES grid-connected inverters to achieve reactive voltage control. In the future, more flexible resources can be utilized to assist the DN system in voltage regulation control, to achieve comprehensive research.

Funding

The research is supported by the Yunnan Power Grid Co., Ltd. Yuxi Power Supply Bureau. Project number: YNKJXM20222420. Project Name: Key Technologies for Fault Localization and Isolation in Incomplete Information Active Distribution Networks Research Topic 2: Analysis of Fault Characteristics Data and Research on Typical Fault Testing Methods in Active Distribution Networks.

References

- Addayo, O., & Yskandar, H. (2023). Maximizing the integration of a battery energy storage system–photovoltaic distributed generation for power system harmonic reduction: An overview. *Energies*, 16(6), 2549-2560. https://doi.org/10.32604/ee.2023.043.
- Bandewad, G., Datta, K. P., Gawali, B. W., & Pawar, S. N. (2023). Review on discrimination of hazardous gases by smart sensing technology. *Artificial Intelligence and Applications*, 1(2), 86-97. https://doi.org/10.47852/bonviewAIA3202434.
- Bolgaryn, R., Wiemer, J., & Braun, S. M. (2023). Security-constrained active power curtailment considering line temperature and thermal inertia. *IET Generation, Transmission & Distribution*, 17(23), 5183-519. https://doi.org/10.1049/gtd2.13029.
- Cong, M., & Zhao, Y. (2024). Coordinated active-reactive power optimization of a distribution system based on a hyper-heuristic algorithm. *Journal of Physics: Conference Series*, 2820(1), 012106-012118. https://doi.org/10.1088/1742-6596/2820/012106.
- Dao, M-T., Truong, K. H., & Do, D. P. N. (2023). Security-constrained temperature-dependent optimal power flow using hybrid pseudogradient based particle swarm optimization and differential evolution. *International Journal on Electrical Engineering and Informatics*, 15(1), 82-105. https://doi.org/10.15676/ijeei.2023.15.1.6
- Ebrahimi, A., Moradlou, M., & Bigdeli, M. (2024). Optimal siting and sizing of custom power system and smart parking lot in the active distribution network. *IET Renewable Power Generation*, 18(5), 779-795. https://doi.org/10.1049/RPG2.12945.
- Furusawa, H., Nishijima, E., Unno, M., & Horita, Y. (2023). Examination of accuracy verification of prediction of photovoltaic power generation using AutoML. *Journal of Japan Society of Energy and Resources*, 44(3), 152-159. https://doi.org/10.24778/jser.4.3_152.
- Ge, H., Zhang, X., Ma, G., Pang, Y., Liu, X., & Xu, X. (2022). A high-proportion household photovoltaic optimal configuration method based on integrated-distributed energy storage system. *IEEJ Transactions on Electrical and Electronic Engineering*, 17(3), 335-343. https://doi.org/10.1002/tee.23516.
- Hirano, M., Nagahama, H., & Muto, J. (2022). Short-wavelength Bouguer gravity anomaly and active fault distribution in the northeastern Japan arc. *Terra Nova*, 34(1), 47-53. https://doi.org/10.1111/ter.12560.
- Hou, S., & Wang, W. (2024). Fault-line selection method in active distribution networks based on improved multivariate variational mode decomposition and lightweight YOLOv10 network. *Energies*, 17(19), 4958-4958. https://doi.org/10.3390/en17194958.
- Hu, D., & Sun, L. (2023). Integrated planning of an active distribution network and DG integration in clusters considering a novel formulation for reliability assessment. CSEE Journal of Power and

- Energy Systems, 9(2), 561-576. https://doi.org/10.17775/CSEEJPES.2020.00150.
- Hu, R., Wang, W., & Wu, X. (2022). Coordinated active and reactive power control for distribution networks with high penetrations of photovoltaic systems. *Solar Energy*, 231(8), 809-827. https://doi.org/10.1016/j.solener.2021.12.025.
- Igor, P., Marinko, S., & Predrag, M. (2023). A new protection system design of active MV distribution network. *Tehnički vjesnik*, 30(1), 131-137. https://doi.org/10.17559/TV-20220509091610.
- Kaicheng, L., Chen, L., & Xiaoyang, D. (2024). Analysis and modeling of time output characteristics for distributed photovoltaic and energy storage. Energy Engineering, 121(4), 933-949. https://doi.org/10.32604/EE.2023.043658.
- Lan, Y., & Illindala, S. M. (2024). Robust distributed load frequency control for multi-area power systems with photovoltaic and battery energy storage system. *Energies*, 17(22), 5536-5536. https://doi.org/10.3390/en1722553.
- Liao, J., Lin, J., & Wu, G. (2024). Two-layer optimization configuration method for distributed photovoltaic and energy storage systems based on IDEC-K clustering. *Energy Reports*, 11(4), 5172-5188. https://doi.org/10.1016/j.egyr.2024.04.047.
- Liao, W., & Li, P. (2021). Distributed active and reactive power control for wind farms based on ADM. International Journal of Electrical Power & Energy Systems, 129(2), 106799. https://doi.org/10.1016/J.IJEPES.2021.106799.
- Liu, J., & Weng, X. (2024). Active Network Expansion Planning Based on Wasserstein Distance and Dual Relaxation. Energies, 17(12), 3005-3015. https://doi.org/10.3390/en17123005.
- Liu, K., & Liang, C. (2024). Analysis and modeling of time output characteristics for distributed photovoltaic and energy storage. *Energy Engineering*, 121(4), 933-949. https://doi.org/10.32604/ee.2023.043658.
- Liu, K., Liang, C., Dong, X., & Liu, L. (2024). Energy economic dispatch for photovoltaic–storage via distributed event-triggered surplus algorithm. *Energy Engineering*, 121(9), 2621-2637. https://doi.org/10.32604/EE.2024.050001.
- Liu, X., & Wang, H. (2022). Research on fault scenario prediction and resilience enhancement strategy of active distribution network under ice disaster. *International Journal of Electrical Power & Energy Systems*, 135(3), 74-78. https://doi.org/10.1016/j.ijepes.2021.107478.
- Li, H., Li, Z., Wang, B., & Sun, K. (2024). Stochastic Optimal Operation of SOP-Assisted Active Distribution Networks with High Penetration of Renewable Energy Sources. *Sustainability*, 16(13), 5808-5814. https://doi.org/10.3390/su16135808.
- Ma, Z., Wang, R., Pu, D., & Yuan, G. (2024). Coordinated optimization scheme for active distribution networks considering electric vehicle charging and discharging optimization under combined heat and power generation. *Journal of Energy Storage*, 101(PA), 113699-113709. https://doi.org/10.1016/J.EST.2024.113699.
- Mukherjee, M., Roy, B. K. S. (2022). Cost-effective operation risk-driven PMU placement in active distribution network considering channel cost and node reliability. *Arabian Journal for Science and Engineering*, 48(5), 6541-6575. https://doi.org/10.1007/s13369-022-07426-9.
- Nemati, B., Hosseini, S. M. H., & Siah, H. (2024). A cooperative approach for generation and lines expansion planning in microgrid-based active distribution networks. *IET Renewable Power Generation*, 18(15), 3355-3377. https://doi.org/10.1049/rpg2.13142.
- Novoa, L., & Brouwer, J. (2021). Optimal DER allocation in meshed microgrids with grid constraints. *International Journal of Electrical Power & Energy Systems*, 128(10), 67-89. https://doi.org/10.1016/j.ijepes.2021.106789.

- Ning, L. (2022). Active Selection or Passive Distribution: The Moderating Effect of Tutor Selection Model on Doctoral Students' Scientific Research Performance. *China Higher Education Research*, 28(3), 67-73. https://doi.org/10.16298/j.cnki.1004-3667.2022.03.10.
- Pan, Y., Li, Z., Gao, L., Su, X., Chen, J., & Huang, S. (2024). Integrated planning research of active distribution networks considering electric vehicle integration in the context of dual carbon. *Journal of Physics: Conference Series*, 2840(1), 012038-012045. https://doi.org/10.1088/1742-596/2840/012038.
- Prasad, S. (2022). Temperature Dependent Branch Current Based Active Distribution System State Estimation. *Iranian Journal of Science and Technology, Transactions of Electrical Engineering*, 47(2), 695-713. https://doi.org/10.1007/s40998-022-00574-6.
- Sah, P., & Mehta, B. (2021). Mitigation of grid connected distributed solar photovoltaic fluctuations using battery energy storage and microgrid. *International Journal of Power and Energy Conversion*, 12(2), 153-162. https://doi.org/10.1504/IPEC.2021.114487.
- Singh, P., & Palu, I. (2021). State coordinated voltage control in an active distribution network with on-load tap changers and photovoltaic systems. Global Energy Interconnection, 4(2), 117-125. https://10.1016/J.GLOEI.2021.05.005.
- Sheng, P., & Palu, I. (2021). State coordinated voltage control in an active distribution network with on-load tap changers and photovoltaic systems. *Global Energy Interconnection*, 4(2), 117-125. https://doi.org/10.1016/J.GLOEI.2021.05.005.
- Sun, Y., & Gao, J. (2021). Evaluating the reliability of distributed photovoltaic energy system and storage against household blackout. *Global Energy Interconnection*, 4(1), 18-27. https://doi.org/10.1016/j.gloei.2021.03.002
- Velasco-Gómez, S., Pérez-Londoño, S., Mora-Floréz, J. (2023).

 Unbalance compensated distance relay for active distribution networks. *Energy Reports*, 9(S3), 438-446. https://doi.org/10.1016/j.egyr.2022.12.129
- Venkatesan, Y., & Palanivelu, A. (2021). Flower pollination-based optimal placement of distributed generation units in distribution networks. *International Journal of Energy Technology and Policy*, 17(4), 346-365. https://doi.org/10.1504/ijetp.2021.10041987.
- Wagle, R., Sharma, P., Sharma, C., & Amin, M. (2024). Optimal power flow based reactive and active power control to mitigate voltage violations in smart inverter enriched distribution network. *International Journal of Green Energy*, 21(2), 359-375. https://doi.org/10.1080/15435075.2023.196324.
- Xu, Y., Zhao, C., & Xie, S. (2021). Novel Fault Location for High Permeability Active Distribution Networks Based on Improved VMD and S-transform. *IEEE Access, 9, 17662-17671. https://doi.org/10.1109/ACCESS.2021.3052349.
- Xie, S., Zhao, C., & Xu, Y. (2021). Novel Fault Location for High Permeability Active Distribution Networks Based on Improved VMD and S-transform. *IEEE Access*, 9, 17662-17671. https://doi.org/10.1109/ACCESS.2021.3052349
- Yi, L., Li, G., & Chen, K. (2022). Optimal scheduling of intelligent building with photovoltaic energy storage system using competitive mechanism integrated multi-objective optimizer. *Arabian Journal for Science and Engineering*, 47(11), 14641-14655. https://doi.org/10.1007/s13369-022-06831-4
- Zhou, Y., Zhang, Y., Zhu, Y., Huang, W., Chen, S., & Ma, G. (2023). Capacity evaluation of hydropower for accommodating wind-photovoltaic power generation in the dry season. *IET Renewable Power Generation*, 17(14), 3424-3441. https://doi.org/10.1049/rpg2.12858



© 2025. The Author(s). This article is an open access article distributed under the terms and conditions of the Creative Commons Attribution-ShareAlike 4.0 (CC BY-SA) International License (http://creativecommons.org/licenses/by-sa/4.0/)